



**University of
Zurich^{UZH}**

**Zurich Open Repository and
Archive**

University of Zurich
University Library
Strickhofstrasse 39
CH-8057 Zurich
www.zora.uzh.ch

Year: 2012

Activity enhancement of the synthetic syrbactin proteasome inhibitor hybrid and biological evaluation in tumor cells

Archer, Crystal R ; Groll, Michael ; Stein, Martin L ; Schellenberg, Barbara ; Clerc, Jérôme ; Kaiser, Markus ; Kondratyuk, Tamara P ; Pezzuto, John M ; Dudler, Robert ; Bachmann, André S

Abstract: Syrbactins belong to a recently emergent class of bacterial natural product inhibitors that irreversibly inhibit the proteasome of eukaryotes by a novel mechanism. The total syntheses of the syrbactin molecules syringolin A, syringolin B, and glidobactin A have been achieved, which allowed the preparation of syrbactin-inspired derivatives, such as the syringolin A-glidobactin A hybrid molecule (SylA-GlbA). To determine the potency of SylA-GlbA, we employed both in vitro and cell culture-based proteasome assays that measure the subcatalytic chymotrypsin-like (CT-L), trypsin-like (T-L), and caspase-like (C-L) activities. We further studied the inhibitory effects of SylA-GlbA on tumor cell growth using a panel of multiple myeloma, neuroblastoma, and ovarian cancer cell lines and showed that SylA-GlbA strongly blocks the activity of NF-kappa B. To gain more insights into the structure-activity relationship, we cocrystallized SylA-GlbA in complex with the proteasome and determined the X-ray structure. The electron density map displays covalent binding of the Thr1 O-gamma atoms of all active sites to the macrolactam ring of the ligand via ether bonds formation, thus providing insights into the structure-activity relationship for the improved affinity of SylA-GlbA for the CT-L activity compared to those of the natural compounds SylA and GlbA. Our study revealed that the novel synthetic syrbactin compound represents one of the most potent proteasome inhibitors analyzed to date and therefore exhibits promising properties for improved drug development as an anticancer therapeutic.

DOI: <https://doi.org/10.1021/bi300841r>

Posted at the Zurich Open Repository and Archive, University of Zurich

ZORA URL: <https://doi.org/10.5167/uzh-68099>

Journal Article

Originally published at:

Archer, Crystal R; Groll, Michael; Stein, Martin L; Schellenberg, Barbara; Clerc, Jérôme; Kaiser, Markus; Kondratyuk, Tamara P; Pezzuto, John M; Dudler, Robert; Bachmann, André S (2012). Activity enhancement of the synthetic syrbactin proteasome inhibitor hybrid and biological evaluation in tumor cells. *Biochemistry*, 51(34):6880-6888.

DOI: <https://doi.org/10.1021/bi300841r>

Activity Enhancement of Synthetic Syrbactin Proteasome Inhibitor

Hybrid and Biological Evaluation in Tumor Cells

Crystal R. Archer^{†‡1}, Michael Groll[§], Martin L. Stein[§], Barbara Schellenberg^{||2}, Jérôme Clerc^{¶3}, Markus Kaiser[¶], Tamara P. Kondratyuk^{*}, John M. Pezzuto^{*‡}, Robert Dudler^{||}, André S. Bachmann^{*†‡4}

**Department of Pharmaceutical Sciences, College of Pharmacy, University of Hawaii at Hilo, 34 Rainbow Drive, Hilo, Hawaii 96720, U.S.A., †University of Hawaii Cancer Center, 1236 Lauhala Street, University of Hawaii at Manoa, Honolulu, Hawaii 96813, U.S.A., ‡Department of Cell and Molecular Biology, John A. Burns School of Medicine, University of Hawaii at Manoa, 651 Ilalo Street, Honolulu, Hawaii 96813, U.S.A., §Center for Integrated Protein Science at the Department Chemie, Technische Universität München, Lichtenbergstr. 4, 85747 Garching, Germany, ||Zürich-Basel Plant Science Center, Institute of Plant Biology, University of Zürich, Zollikerstr. 107, 8008 Zürich, Switzerland, and ¶Zentrum für Medizinische Biotechnologie, Fakultät Biologie & Fakultät für Chemie, Universität Duisburg-Essen, Universitätsstr. 2, 45141 Essen, Germany*

Present addresses: ¹University of Texas Health Science Center at San Antonio, Department of Biochemistry, San Antonio, Texas 78229, Texas, U.S.A., ²Wellcome Trust Centre for Cell-Matrix Research, Faculty of Life Sciences, University of Manchester, Manchester M13 9PT, U.K., ³Institut für Organische und Biomolekulare Chemie, Universität Göttingen, Tammannstr. 2, 37077 Göttingen, Germany.

⁴To whom correspondence should be addressed at *Department of Pharmaceutical Sciences, College of Pharmacy, University of Hawaii at Hilo, 34 Rainbow Drive, Hilo, HI 96720, U.S.A. Tel: +808-933-2807; Fax: +808-933-2974; E-mail: andre@hawaii.edu*

ABSTRACT

Syrbactins belong to a recently emerged class of bacterial natural product inhibitors that irreversibly inhibit the proteasome of eukaryotes by a novel mechanism. The total syntheses of the syrbactin molecules syringolin A, syringolin B, and glidobactin A have been achieved which enabled the preparation of syrbactin-inspired derivatives, such as the syringolin A/glidobactin A hybrid molecule SylA-GlbA. To determine the potency of SylA-GlbA, we employed both *in vitro* and cell culture-based proteasome assays that measure the sub-catalytic chymotrypsin-like (CT-L), trypsin-like (T-L), and caspase-like (C-L) activities. We further studied the inhibitory effects of SylA-GlbA on tumor cell growth, using a panel of multiple myeloma, neuroblastoma, and ovarian cancer cell lines and showed that SylA-GlbA strongly blocks the activity of NF- κ B. To gain more insights into the structure-activity relationship, we co-crystallized the SylA-GlbA compound in complex with the proteasome and determined the X-ray structure. The electron density map displays covalent binding of the Thr-10^y of all active sites to the macrolactam ring of the ligand via ether bond formation, thus providing insights into the structure-activity relationship for the improved affinity of SylA-GlbA for the CT-L activity compared to the natural compounds SylA and GlbA. Our study revealed that the novel synthetic syrbactin compound represents one of the most potent proteasome inhibitors analyzed to date and therefore exhibits promising properties for an improved drug development as an anti-cancer therapeutic.

Key words: cancer; co-crystallization; NF- κ B; proteasome inhibitor; structure-activity relationship; syrbactin analog

INTRODUCTION

Syrbactins are natural product small molecules that include the syringolins and glidobactins. While syringolins were identified more recently in isolates from the plant pathogen *Pseudomonas syringae* pv. *syringae* (*Pss*) (1), the structurally-related glidobactins were discovered in the 1980's from an unknown species of the order Burkholderiales (2-5). Syringolin A (SylA) and glidobactin A (GlbA) represent the predominant forms in these bacterial pathogens, whereas SylB-F and GlbB-F are naturally occurring syrbactin variants expressed in minor quantities (1, 6, 7).

In 2006, we demonstrated that the plant pathogen-derived natural product SylA induces massive p53 accumulation followed by apoptosis in neuroblastoma and ovarian cancer cells (8). Two years later, we discovered that SylA represents a bacterial virulence factor that irreversibly inhibits the eukaryotic proteasome by a novel mechanism (9). The proteasome is a multi-protein complex that is responsible for intracellular protein degradation, both via ubiquitin-dependent and ubiquitin-independent proteolysis (10-13). Many of these proteasome-controlled proteins regulate cell division, proliferation, and apoptosis and proteasome inhibitors represent a promising family of anti-neoplastic agents (12-19). Bortezomib (Velcade®) is the first proteasome inhibitor approved by the U.S. Food and Drug Administration (FDA) for the treatment of refractory and/or relapsed multiple myeloma (MM) and mantle cell lymphoma and preclinical studies have validated a number of next-generation proteasome inhibitors such as carfilzomib (PR-171), marizomib (NPI-0052), and MLN9708 (13).

Despite its success on the market, bortezomib therapy has several disadvantages, including intravenous administration and multiple side-effects such as thrombocytopenia, neutropenia, and gastrointestinal disorders. Bortezomib also leads to severe but reversible neurodegenerative

effects and triggers nerve degeneration by exhibiting substantial off-target activity (12). Additional challenges are the increasing chemoresistance and patient relapse in response to proteasome inhibitors and one novel approach may be to target the immunoproteasome, a proteasomal variant found predominantly in cells of hematopoietic origin that differs from the constitutive proteasome found in most other cell types (20). Indeed, the recent elucidation of the immune- and constitutive proteasome crystal structures revealed important differences in substrate and inhibitor specificity (21), thus providing new insights into the structure-guided design of novel lead structures selective for the immunoproteasome and sub-catalytic proteasome activities.

We previously showed that SylA inhibits the chymotrypsin-like (CT-L), trypsin-like (T-L), and caspase-like (C-L) sub-catalytic activities of the proteasome, while GlbA inhibits the CT-L and T-L, but not C-L sub-catalytic activities (9). In 2009, the chemical synthesis of syringolin A and syringolin B was achieved (22), which spurred the subsequent synthesis of novel syringolin- and glidobactin-inspired syrbactin analogs (23-27). Of those, SylA-LIP and TIR-203 represent two novel analogs with improved biological activities (24, 27). Most recently, we synthesized the hybrid molecule SylA-GlbA (Fig.1) consisting of a SylA macrocycle connected to the lipophilic GlbA side chain and demonstrated that the SylA or GlbA macrocycle moiety has critical influence on the $\beta 1$ (C-L) subsite selectivity (28). To further evaluate the potency of this novel syrbactin analog, we performed a biological characterization of SylA-GlbA and determined the complex structure of the ligand with the proteasome in order to gain additional insights into inherent structure-activity relationships.

1
2
3
4
5
6
7
8
9
10
11
12
13
14
15
16
17
18
19
20
21
22
23
24
25
26
27
28
29
30
31
32
33
34
35
36
37
38
39
40
41
42
43
44
45
46
47
48
49
50
51
52
53
54
55
56
57
58
59
60

EXPERIMENTAL PROCEDURES

Synthesis and natural product isolation of syrbactins. The SylA-GlbA hybrid (SylA-GlbA) and synthetic SylA were synthesized as previously reported (22, 28, 29). GlbA was isolated from its biological source as described (1, 30, 31). All compounds were dissolved in sterile DMSO and frozen in aliquots at -20° C. At the beginning of each experiment, aliquots were thawed and diluted to the final concentration.

Mammalian cell cultures and reagents. The following panel of chemosensitive and chemoresistant cancer cell lines was used in this study. The human neuroblastoma (NB) cell line SK-N-SH was obtained from the American Type Culture Collection (ATCC) (32). Multiple myeloma (MM) cell lines MM1.S and MM1.RL are sensitive and resistant to dexamethasone, respectively. U266 is an IL-6 producing cell line isolated from the peripheral blood of a male myeloma patient. All myeloma cells were provided by N. Krett (Northwestern University) (33). The human ovarian cancer cell line SKOV3, which is resistant to several cytotoxic drugs was available at the University of Hawaii Cancer Center (34, 35). Cells were seeded 18-24 hours before syrbactin or bortezomib treatments and analyzed after 24-72 hours. Human embryonic kidney 293/NF-κB-Luc cell line was designed for monitoring the activity of the NF-κB and was purchased from Panomics (Freemont, CA, USA). This cell line contains chromosomal integration of a luciferase reporter construct regulated by the NF-κB response element. Transcription factors can bind to the response element when stimulated by certain agents, allowing transcription of the luciferase gene. *N*-tosyl-L-phenylalanyl chloromethyl ketone (TPCK) was purchased from Santa Cruz Biotechnology, Inc. (Santa Cruz, CA, USA), (*E*)-3-(4-

Methylphenylsulfonyl)-2-propenenitrile (BAY-11) was purchased from Cayman Chemical (Ann Arbor, MI, USA). Bortezomib was purchased from LC Laboratories (Woburn, MA, USA).

In vitro proteasome activity assay. *In vitro* proteasome inhibition assays were performed in 96-well microtiter plates with human erythrocyte 20S proteasomes using the Assay Kit for Drug Discovery AK-740 (Biomol). Reactions were performed at 37 °C in 100 µl volumes containing a serial dilution of SylA-GlbA, 2 µg/ml 20S proteasome and 100 µM Suc-LLVY-AMC, Boc-LRR-AMC or Z-LLE-AMC for assaying the chymotrypsin-like, trypsin-like and caspase-like activity, respectively, according to instructions of the manufacturer. Fluorescence was monitored with an MWGt Sirius HT plate reader (BIO-TEK® Instruments) equipped with 360 nm excitation and 460 nm emission filters.

In vivo proteasome activity assay. The cell culture-based *in vivo* proteasome-Glo activity assay was performed as previously described (9, 24). Clear-bottom, white-walled 96-well microtiter cell culture plates (Greiner Bio-One North America Inc., Monroe, NC, USA), were seeded with cells as indicated and treated with syrbactin or bortezomib. Proteasome inhibition was measured using the proteasome Glo™ reagent according to the manufacturer's instructions (Promega, Madison, WI, USA). In brief, cancer cells were treated with SylA-GlbA, GlbA, SylA or bortezomib at different concentrations as indicated, and incubated for 2 hours. After incubation, cells were incubated for 15 min with 100 µl of proteasome Glo reagent, which permeabilizes cells and contains the bioluminescent substrates Suc-LLVY-aminoluciferin, Z-nLPnLD-aminoluciferin, and Z-LRR-aminoluciferin to determine the chymotrypsin-like (CT-L),

caspase-like (C-L), and trypsin-like (T-L) activities, respectively. The luminescence was measured with a Dynex MLX luminometer.

Cell proliferation assay. The CellTiter 96 Aqueous One solution Cell Proliferation Assay (2-(4,5-dimethylthiazol-2-yl)-5-(3-carboxymethoxyphenyl)-2-(4-sulfophenyl)-2H-tetrazolium, inner salt; MTS) (Promega, San Luis Obispo, CA, USA) measures metabolic cell activity and was used to indirectly determine the viability of cells after 48 hours treatment with SylA-GlbA at indicated concentrations (0-1 μ M) by measuring the absorbance at 492 nm using a Perkin Elmer HTS7000 Plus bioassay reader. The IC₅₀ values in Table 1 were calculated by setting the lowest dose at 100%, using 3PL curve fitting in Prism from GraphPad Software, Inc (La Jolla, CA).

NF- κ B activity assay. The NF- κ B activity assay was performed as previously described (36). Briefly, HEK293/NF- κ B-Luc cells were seeded into sterile white-walled 96-well plates at 2×10^4 cells per well in Dulbecco's modified media with 10% FBS. After growing cells for 48 hr to 90% confluence, the medium was replaced with fresh medium containing tumor necrosis factor alpha (TNF- α) (final concentration 30 ng/ml) and cells were treated simultaneously for 6 hr with inhibitor compounds (SylA-GlbA, SylA, and GlbA) at various concentrations. To avoid false-positive responses, a cytotoxicity control experiment was included in parallel to ensure that the NF- κ B activity changes within the 6 hr incubation period are not due to cell death (data not shown). Luciferase activity was determined with a luciferase kit from Promega (Madison, WI, USA) according to the manufacturer's instructions. Following treatment, the cells were washed with phosphate-buffered saline and 50 μ L of 1x Reporter lysis buffer was added before plates were placed in a -80° C freezer. The following day, the cells were thawed and assayed for luciferase activity with a LUMIstar Galaxy Luminometer (BMG Labtechnologies, Durham, NC,

USA). As a positive control, two NF- κ B inhibitors were used: *N*-tosyl-L-phenylalanyl chloromethyl ketone (TPCK) and (*E*)-3-(4-Methylphenylsulfonyl)-2-propenenitrile (BAY-11). Results were expressed as a percentage relative to control (TNF α -treated) samples, and dose-response curves were constructed for the determination of IC₅₀ values, which were generated from the results of eight serial dilutions of inhibitor compounds. Data represent the mean of two independent experiments, each performed in triplicate (n=6).

Co-crystallization. Crystals of the 20S proteasome from *S. cerevisiae* were grown in hanging drops at 20° C as already has been described (37) and incubated for 48 hours with the chemical compound SylA-GlbA at 10 mM. The protein concentration used for crystallization was 45 mg/ml in Tris-HCl (10 mM, pH 7.5) and EDTA (1 mM). The drops contained 1 μ l of protein and 1 μ l of the reservoir solution, containing 20 mM of magnesium acetate, 100 mM of morpholino-ethane-sulphonic acid (pH 6.9) and 10% of MPD.

The space group belongs to P2₁ with cell dimensions of $a = 135.9 \text{ \AA}$, $b = 298.8 \text{ \AA}$, $c = 145.3 \text{ \AA}$ and $\beta = 112.6^\circ$ (see Table S1). Data to 2.8 \AA for the proteasome:inhibitor-complex were collected using synchrotron radiation with $\lambda = 1.0 \text{ \AA}$ at the X06SA-beamline in SLS/Villingen/Switzerland. Crystals were soaked in a cryoprotecting buffer (30% MPD, 20 mM of magnesium acetate, 100 mM of morpholino-ethane-sulfonic acid pH 6.9) and frozen in a stream of liquid nitrogen gas at 100 K (Oxford Cryo Systems). X-ray intensities were evaluated by using XDS program package (38). The anisotropy of diffraction was corrected by an overall anisotropic temperature factor by comparing observed and calculated structure amplitudes using the program CNS (39, 40). The electron density map was improved by averaging and back transforming the reflections 10 times over the twofold non-crystallographic symmetry axis using

the program package MAIN (41). Conventional crystallographic rigid body, positional and temperature factor refinements were carried out with CNS using the yeast 20S proteasome structure as starting model (42). Modelling experiments were performed with the program MAIN. Apart from the bound inhibitor molecules, structural changes were only noted in the specificity pockets. Temperature factor refinement indicates full occupancies of all inhibitor binding sites. The inhibitors have been omitted for phasing. The refined proteasome:SylA-GlbA-complex structures revealed current crystallographic values of $R_{\text{cryst}} = 0.212$, $R_{\text{free}} = 0.237$ (43) (Table S1).

RESULTS

SylA-GlbA inhibits all three catalytic activities of the proteasome. In an effort to generate more effective SylA analogs that exhibit higher potency, we recently synthesized a hybrid molecule that combines SylA with properties of GlbA (28). As shown in Fig. 1, the hybrid molecule SylA-GlbA is built up from the SylA macrocycle connected to the GlbA side chain. To determine the resulting inhibitory properties of this hybrid molecule, we employed an *in vitro* proteasome assay. In this assay, SylA-GlbA inhibited the chymotrypsin-like (CT-L) activity with an apparent K_i of 12.5 ± 1.5 nM, the trypsin-like (T-L) with an apparent K_i of 136.9 ± 12.4 nM, and the caspase-like (C-L) activity with an apparent K_i of 3.7 ± 1.2 μ M, thereby demonstrating that the proteasome inhibitor SylA-GlbA is one of the most potent syrbactins reported to date.

To corroborate the *in vitro* analysis, we tested the effectiveness of SylA-GlbA in a cell culture-based system that allows the detection of each sub-catalytic proteasome activity *in vivo*. As shown in Fig. 2, SylA-GlbA inhibited the CT-L, T-L, and C-L activities in a dose-dependent

manner, in five cancer cell lines representing multiple myeloma (MM1.S, MM1.RL, U266), neuroblastoma (SK-N-SH), and ovarian cancer (SKOV3). The syrbactin GlbA inhibited the proteasomal activities in a similar fashion. SylA and bortezomib were included as controls and tested in two cell lines (SK-N-SH and SKOV3). While SylA showed an expected weaker response with highest inhibitory effects against the CT-L activity of the proteasome, the FDA-approved proteasome inhibitor bortezomib (Velcade) strongly inhibited the three catalytic activities in these two cell lines, with highest potency against the CT-L activity.

SylA-GlbA inhibits the proliferation of cancer cells more effectively than SylA. To examine the effect of SylA-GlbA-induced proteasome inhibition on cancer cell proliferation, we tested five cancer cell lines in the presence of increasing inhibitor concentrations (Fig. 3). The inhibitory effect of SylA-GlbA was most prominent in multiple myeloma MM1.S cells and equally potent in dexamethasone-resistant multiple myeloma MM1.RL cells. SylA-GlbA also decreased the cell viability of multiple myeloma U266 cells, ovarian cancer SKOV3 cells, and neuroblastoma SK-N-SH cells in a dose-dependent fashion. At concentrations of 0.1 μ M or higher, cell growth inhibition was 100% in both multiple myeloma cell lines MM1.S and MM1.RL. The concentration at which cell growth is inhibited by 50% (IC_{50}) was calculated (Table 1) and determined at 28 nM (MM1.S), 27 nM (MM1.RL), 45 nM (U266), 109 nM (SKOV3), and 321 nM (SK-N-SH). In contrast, the IC_{50} values previously reported for SylA are between 9 μ M and 39 μ M (depending on cancer cell line) (8, 24), thus confirming that the novel hybrid syrbactin SylA-GlbA exhibits significantly more potent (100- to 2,000-fold) anti-proliferative activity than SylA.

Syrbactins inactivate TNF- α induced NF- κ B activity. To determine whether NF- κ B inactivation might be the underlying mechanism of proteasome inhibitor-induced cell death, three syrbactins (SylA-GlbA, SylA, and GlbA) were tested in a cell culture-based NF- κ B transcription factor assay using stably transfected HEK293/NF- κ B-Luc cells. As shown in Table 2, the hybrid molecule SylA-GlbA strongly inhibited the TNF- α stimulated NF- κ B activity and was more potent than SylA or GlbA. Of note, the IC₅₀ value of SylA-GlbA (2.87 μ M) was comparable with those of well-established NF- κ B inhibitors TPCK (4.2 μ M) and BAY-11 (2.6 μ M) which were included as controls. These results demonstrate for the first time that similar to bortezomib, syrbactin-promoted proteasome blockage results in the inhibition of NF- κ B activity, which then leads to apoptosis as we previously demonstrated (8, 24).

Crystal structure of SylA-GlbA with the yeast 20S proteasome. In comparison with the natural product SylA the synthetic SylA-GlbA analog revealed significantly decreased IC₅₀ values for all three proteolytically active sites of approximately three orders of magnitude. Hence, we performed crystal structure analysis of SylA-GlbA in complex with the yeast proteasome at 2.8 Å resolution ($R_{\text{free}}=24.4\%$) for characterizing the ligand at the molecular level in comparison to SylA and GlbA. The electron density map displays the macrolactam ring of the SylA-GlbA-ligand covalently bound to the Thr-10 γ by formation of an irreversible ether bond formation (Fig. 4A,B). The oxyanion-hole is occupied by the carbonyl-oxygen of the reactive 1,4-Michael head group of the ligand. The SylA-GlbA peptide moiety adopts the formation of an antiparallel β -sheet in the non-primed substrate binding channel as observed previously (44). Furthermore, in the case of the CT-L and TL-active site the peptide backbone is also stabilized by hydrogen bond formation with Asp114 located on the adjacent subunit either being β 6 or β 2,

respectively. Of note, this additional stabilization is absent in the substrate binding channel forming the C-L site and explains the reduced affinity of SylA, GlbA and SylA-GlbA for the latter. Substantial variations in the binding probability between the CT-L, T-L and C-L activities are caused by the molecular flexibility of the distinct specificity pockets in respect to entropic and enthalpic ligand stabilization, thus being a prime cause for the preference of the syrbactins to predominantly block the CT-L site.

Interestingly, although the structural superposition of the macrolactom rings of SylA, GlbA and SylA-GlbA match almost perfectly (r.m.s.d. < 0.2 Å; Fig. 4C), there exist major differences in the binding affinity between SylA versus GlbA and SylA-GlbA. This discrepancy can be explained that: i) SylA harbors an isopropyl side chain in P4, which, however due to the presence of a urea-moiety between P3 and P4, is out of frame and therefore performs only impaired interactions with the S4 specificity pocket; ii) the N-terminal aliphatic fatty acid chains in GlbA and SylA-GlbA, which point towards the adjacent subunit β_6 in the CT-L substrate binding channel, gets stabilized in an apolar pocket (Fig. 4A). Remarkably, although the lipophilic tails between GlbA and SylA-GlbA differ in their orientation (Fig. 4C), the *in vitro* IC₅₀ values of the natural product and the SylA-GlbA compound are quite similar. Thus, the strong binding affinity of GlbA and SylA-GlbA compared to SylA can be explained by the presence of the aliphatic linker which is flexible in solution but is bound to hydrophobic patches of the central hydrolytic proteasomal chamber upon ligand docking to the proteolytic centre. As a result and in contrast to SylA, this additional stabilization of GlbA as well as SylA-GlbA at the active site vicinity increases the mean residence time of the ligands and therefore allows completion of the irreversible ether-bond formation with the Thr1O^γ.

DISCUSSION

Natural products involved in plant-pathogen interactions can serve as an inspiring source for the identification of new bioactive entities as well as provide strategies on how to achieve small molecule manipulation of biological systems (45). Syrbactin is a subordinate term for the syringolin, glidobactin, and cepafungin natural product families and their grouping is based on their related molecular frameworks, similar biosynthesis pathways, and identical modes-of-action, being irreversible proteasome inhibition (46). Syrbactins are now recognized as a new, and structurally distinct class of proteasome inhibitors (15), which prompted the design of synthetic syrbactin-inspired analogs (23-27).

Our study demonstrates that the synthetic hybrid molecule SylA-GlbA is a potent proteasome inhibitor and inhibits the three sub-catalytic activities in a dose-dependent manner and at concentrations comparable with bortezomib. SylA-GlbA also substantially inhibits the proliferation of several cancer cell lines, with most potent effects in multiple myeloma. While proteasome inhibition is a validated strategy for therapy of multiple myeloma, relapse is common and often associated with chemoresistance. Therefore, the identification of novel compounds that overcome resistance to conventional drugs as well as nonspecific proteasome inhibitors is increasingly important (20). Intriguingly, the dexamethasone-sensitive (MM1.S) and dexamethasone-resistant (MM1.RL) multiple myeloma cell lines were both inhibited by SylA-GlbA in the nanomolar range with IC_{50} values at 28 nM and 27 nM, respectively, suggesting that SylA-GlbA is equally effective in multiple myeloma cells that exhibit chemoresistance to a conventional drug. In contrast, the (wild type) SylA was significantly less potent in both multiple myeloma cell lines and cell treatments required about five-fold higher drug concentrations in

dexamethasone-resistant cells to achieve comparable growth inhibition (8.5 μ M and 39.3 μ M, respectively) (24).

The NF- κ B transcription factor plays an important role in tumorigenesis through induction of cell proliferation, suppression of apoptosis, metastasis, and induction of angiogenesis (47). Bortezomib inhibits NF- κ B activity, the mechanism attributed to its antitumor actions, which led to its approval by the Food and Drug Administration (FDA) in 2003 for the treatment of multiple myeloma. Based on our findings, syrbactins inactivate TNF- α activated NF- κ B in stably transfected HEK293/NF- κ B-Luc cells at micromolar concentrations, with highest potency in multiple myeloma.

Given the large number of substrates of the proteasome, it seems surprising that inhibition of NF- κ B activity should be the only mechanism by which proteasome inhibitors exert their anti-tumor effects. Indeed, other proteasome inhibitors including clasto-lactacystin do not lead to I κ B accumulation in the cytoplasm and nuclear loss of NF- κ B and therefore do not inhibit NF- κ B activity (48, 49). Moreover, a paradigm shift was recently introduced proposing that NF- κ B inhibition might be irrelevant to the effects of bortezomib in multiple myeloma cells and involves other signaling routes and proteasome-independent degradation of I κ B α (50, 51). The possible activation of distinct and cell-type specific downstream cell signaling events in response to proteasome inhibition might also explain why SylA-GlbA treatments were most effective in multiple myeloma cells (Fig. 3), despite the fact that the inhibition of proteasomal activities by SylA-GlbA was similar in all five tested cell lines (Fig. 2).

The structural evaluation of SylA, GlbA and SylA-GlbA suggests an improved binding probability starting from a charged and highly polar moiety adjacent to the macrolactam scaffold in SylA with impaired binding affinity and continuing with an enhanced decoration as well as

1
2
3 exploitation of the distant hydrophobic pocket by an aliphatic linker that eventually can further
4
5 be optimized with maximum inhibition values for future syrbactin-derivatives. Thus, the
6
7 structural elucidation of the SylA-GlbA-complex and its comparison with SylA and GlbA
8
9 facilitates novel innovations *via* fragment-based drug design strategies to discover new chemical
10
11 entities as demonstrated by the aliphatic linker of either the natural product GlbA or its synthetic
12
13 derivative SylA-GlbA.
14
15

16
17 In summary, we have characterized the novel synthetic syrbactin analog SylA-GlbA that
18
19 incorporates unique structural features of both SylA and GlbA, creating a hybrid molecule that
20
21 exhibits enhanced biological activity over other syrbactin compounds and is comparable with
22
23 well-studied proteasome inhibitors such as the FDA-approved bortezomib used in the clinic. It is
24
25 tempting to speculate that syrbactins could similarly be developed into a drug for the treatment
26
27 of multiple myeloma and likely other types of cancer. To achieve this, further development of
28
29 next-generation syrbactin analogs will be important in an endeavor to create other clinically
30
31 relevant proteasome inhibitors that may be used to achieve therapeutic synergisms or as
32
33 replacement therapies for bortezomib-chemoresistant multiple myeloma and other forms of
34
35 cancer (17).
36
37
38
39
40
41
42
43
44

45 46 **ACKNOWLEDGEMENTS**

47
48 We are grateful to Prof. Dr. Nancy L. Krett (Northwestern University, Chicago, IL, USA) for
49
50 providing multiple myeloma cells (MM1.S, MM1.RL, and U266). Dr. Dana-Lynn Koomoa and
51
52 Erin Mitsunaga are thanked for initial contributions to this project and Richard Feicht for yeast
53
54
55
56
57
58
59
60

proteasome purification. We acknowledge the staff of the Beamlines X06SA and X06DA at the Paul Scherrer Institute, SLS, Villingen, Switzerland for their support during data collection.

FUNDING

This work was supported by the Robert C. Perry Fund of the Hawaii Community Foundation (HCF grant # 10ADVC-47862, A.S.B) and the Hawaii Business and Acceleration Mentors (HiBEAM, A.S.B). Further support was provided by an ERC Starting Grant (ERC grant agreement # 258413, M.K.), the Swiss National Science Foundation (grant # 31003A-134936, R.D.), and the German-Israeli Foundation for Scientific Research and Development (GIF grant # 1102/2010, M.G.).

REFERENCES

1. Amrein, H., Makart, S., Granado, J., Shakya, R., Schneider-Pokorny, J., and Dudler, R. (2004) Functional analysis of genes involved in the synthesis of syringolin A by *Pseudomonas syringae* pv. *syringae* B301 D-R, *Mol Plant Microbe Interact* 17, 90-97.
2. Oka, M., Nishiyama, Y., Ohta, S., Kamei, H., Konishi, M., Miyaki, T., Oki, T., and Kawaguchi, H. (1988) Glidobactins A, B and C, new antitumor antibiotics. I. Production, isolation, chemical properties and biological activity, *J Antibiot (Tokyo)* 41, 1331-1337.

3. Oka, M., Numata, K., Nishiyama, Y., Kamei, H., Konishi, M., Oki, T., and Kawaguchi, H. (1988) Chemical modification of the antitumor antibiotic glidobactin, *J Antibiot (Tokyo)* 41, 1812-1822.
4. Oka, M., Ohkuma, H., Kamei, H., Konishi, M., Oki, T., and Kawaguchi, H. (1988) Glidobactins D, E, F, G and H; minor components of the antitumor antibiotic glidobactin, *J Antibiot (Tokyo)* 41, 1906-1909.
5. Oka, M., Yaginuma, K., Numata, K., Konishi, M., Oki, T., and Kawaguchi, H. (1988) Glidobactins A, B and C, new antitumor antibiotics. II. Structure elucidation, *J Antibiot (Tokyo)* 41, 1338-1350.
6. Waspi, U., Blanc, C., Winkler, C., Ruedi, P., and Dudler, R. (1998) Syringolin, a novel peptide elicitor from *Pseudomonas syringae* pv. *syringae* that induces resistance to *Pyricularia oryzae* in rice, *Mol Plant Microbe Interact* 11, 727-733.
7. Waspi, U., Hassa, P., Staempfli, A. A., Molleyres, L. P., Winker, T., and Dudler, R. (1999) Identification and structure of a family of syringolin variants: unusual cyclic peptides from *Pseudomonas syringae* pv. *syringae* that elicit defense responses in rice, *Microbiol Res* 154, 89-93.
8. Coleman, C. S., Rocetes, J. P., Park, D. J., Wallick, C. J., Warn-Cramer, B. J., Michel, K., Dudler, R., and Bachmann, A. S. (2006) Syringolin A, a new plant elicitor from the phytopathogenic bacterium *Pseudomonas syringae* pv. *syringae*, inhibits the proliferation of neuroblastoma and ovarian cancer cells and induces apoptosis, *Cell Prolif* 39, 599-609.
9. Groll, M., Schellenberg, B., Bachmann, A. S., Archer, C. R., Huber, R., Powell, T. K., Lindow, S., Kaiser, M., and Dudler, R. (2008) A plant pathogen virulence factor inhibits the eukaryotic proteasome by a novel mechanism, *Nature* 452, 755-758.

10. Adams, J. (2003) The proteasome: structure, function, and role in the cell, *Cancer Treat Rev 29 Suppl 1*, 3-9.
11. Chitra, S., Nalini, G., and Rajasekhar, G. (2012) The ubiquitin proteasome system and efficacy of proteasome inhibitors in diseases, *Int J Rheum Dis 15*, 249-260.
12. Huber, E. M., and Groll, M. (2012) Inhibitors for the Immuno- and Constitutive Proteasome: Current and Future Trends in Drug Development, *Angew Chem Int Ed Engl*, In Press.
13. Moreau, P., Richardson, P. G., Cavo, M., Orlowski, R. Z., San Miguel, J. F., Palumbo, A., and Harousseau, J. L. (2012) Proteasome inhibitors in multiple myeloma: ten years later, *Blood*, In Press.
14. Adams, J. (2004) The proteasome: a suitable antineoplastic target, *Nat Rev Cancer 4*, 349-360.
15. Kisselev, A. F. (2008) Joining the army of proteasome inhibitors, *Chem Biol 15*, 419-421.
16. Kisselev, A. F., and Goldberg, A. L. (2001) Proteasome inhibitors: from research tools to drug candidates, *Chem Biol 8*, 739-758.
17. Orlowski, R. Z., and Kuhn, D. J. (2008) Proteasome inhibitors in cancer therapy: lessons from the first decade, *Clin Cancer Res 14*, 1649-1657.
18. Rajkumar, S. V., Richardson, P. G., Hideshima, T., and Anderson, K. C. (2005) Proteasome inhibition as a novel therapeutic target in human cancer, *J Clin Oncol 23*, 630-639.
19. Voorhees, P. M., Dees, E. C., O'Neil, B., and Orlowski, R. Z. (2003) The proteasome as a target for cancer therapy, *Clin Cancer Res 9*, 6316-6325.

- 1
2
3
4
5
6
7
8
9
10
11
12
13
14
15
16
17
18
19
20
21
22
23
24
25
26
27
28
29
30
31
32
33
34
35
36
37
38
39
40
41
42
43
44
45
46
47
48
49
50
51
52
53
54
55
56
57
58
59
60
20. Kuhn, D. J., Hunsucker, S. A., Chen, Q., Voorhees, P. M., Orlowski, M., and Orlowski, R. Z. (2009) Targeted inhibition of the immunoproteasome is a potent strategy against models of multiple myeloma that overcomes resistance to conventional drugs and nonspecific proteasome inhibitors, *Blood* 113, 4667-4676.
21. Huber, E. M., Basler, M., Schwab, R., Heinemeyer, W., Kirk, C. J., Groettrup, M., and Groll, M. (2012) Immuno- and constitutive proteasome crystal structures reveal differences in substrate and inhibitor specificity, *Cell* 148, 727-738.
22. Clerc, J., Groll, M., Illich, D. J., Bachmann, A. S., Huber, R., Schellenberg, B., Dudler, R., and Kaiser, M. (2009) Synthetic and structural studies on syringolin A and B reveal critical determinants of selectivity and potency of proteasome inhibition, *Proc Natl Acad Sci U S A* 106, 6507-6512.
23. Anshu, A., Thomas, S., Agarwal, P., Ibarra-Rivera, T. R., Pirrung, M. C., and Schonthal, A. H. (2011) Novel proteasome-inhibitory syrbactin analogs inducing endoplasmic reticulum stress and apoptosis in hematological tumor cell lines, *Biochem Pharmacol* 82, 600-609.
24. Archer, C. R., Koomoa, D. L., Mitsunaga, E. M., Clerc, J., Shimizu, M., Kaiser, M., Schellenberg, B., Dudler, R., and Bachmann, A. S. (2010) Syrbactin class proteasome inhibitor-induced apoptosis and autophagy occurs in association with p53 accumulation and Akt/PKB activation in neuroblastoma, *Biochem Pharmacol* 80, 170-178.
25. Clerc, J., Schellenberg, B., Groll, M., Bachmann, A. S., Huber, R., Dudler, R., and Kaiser, M. (2010) Convergent synthesis and biological evaluation of Syringolin A and derivatives as eukaryotic 20S proteasome inhibitors, *Eur J Org Chem* 21, 3991-4003.

26. Ibarra-Rivera, T. R., Opoku-Ansah, J., Ambadi, S., Bachmann, A. S., and Pirrung, M. C. (2011) Syntheses and cytotoxicity of syringolin B-based proteasome inhibitors, *Tetrahedron* 67, 9950-9956.
27. Opoku-Ansah, J., Ibarra-Rivera, T. R., Pirrung, M. C., and Bachmann, A. S. (2012) Syringolin B-inspired proteasome inhibitor analogue TIR-203 exhibits enhanced biological activity in multiple myeloma and neuroblastoma, *Pharm Biol* 50, 25-29.
28. Clerc, J., Li, N., Krahn, D., Groll, M., Bachmann, A. S., Florea, B. I., Overkleeft, H. S., and Kaiser, M. (2011) The natural product hybrid of Syringolin A and Glidobactin A synergizes proteasome inhibition potency with subsite selectivity, *Chem Commun (Camb)* 47, 385-387.
29. Clerc, J., Florea, B. I., Kraus, M., Groll, M., Huber, R., Bachmann, A. S., Dudler, R., Driessen, C., Overkleeft, H. S., and Kaiser, M. (2009) Syringolin A selectively labels the 20 S proteasome in murine EL4 and wild-type and bortezomib-adapted leukaemic cell lines, *Chembiochem* 10, 2638-2643.
30. Schellenberg, B., Bigler, L., and Dudler, R. (2007) Identification of genes involved in the biosynthesis of the cytotoxic compound glidobactin from a soil bacterium, *Environ Microbiol* 9, 1640-1650.
31. Waspi, U., Schweizer, P., and Dudler, R. (2001) Syringolin reprograms wheat to undergo hypersensitive cell death in a compatible interaction with powdery mildew, *Plant Cell* 13, 153-161.
32. Biedler, J. L., Helson, L., and Spengler, B. A. (1973) Morphology and growth, tumorigenicity, and cytogenetics of human neuroblastoma cells in continuous culture, *Cancer Res* 33, 2643-2652.

- 1
2
3
4
5
6
7
8
9
10
11
12
13
14
15
16
17
18
19
20
21
22
23
24
25
26
27
28
29
30
31
32
33
34
35
36
37
38
39
40
41
42
43
44
45
46
47
48
49
50
51
52
53
54
55
56
57
58
59
60
33. Greenstein, S., Krett, N. L., Kurosawa, Y., Ma, C., Chauhan, D., Hideshima, T., Anderson, K. C., and Rosen, S. T. (2003) Characterization of the MM.1 human multiple myeloma (MM) cell lines: a model system to elucidate the characteristics, behavior, and signaling of steroid-sensitive and -resistant MM cells, *Exp Hematol* 31, 271-282.
34. Fogh, J., and Trempe, G. (1975) New human tumor cell lines, In *Human Tumor Cells In Vitro* (Fogh, J., Ed.), p 155, Plenum Press, New York.
35. Fogh, J., Wright, W. C., and Loveless, J. D. (1977) Absence of HeLa cell contamination in 169 cell lines derived from human tumors, *J Natl Cancer Inst* 58, 209-214.
36. Kondratyuk, T. P., Park, E. J., Yu, R., van Breemen, R. B., Asolkar, R. N., Murphy, B. T., Fenical, W., and Pezzuto, J. M. (2012) Novel marine phenazines as potential cancer chemopreventive and anti-inflammatory agents, *Mar Drugs* 10, 451-464.
37. Groll, M., and Huber, R. (2005) Purification, crystallization and X-ray analysis of the yeast 20S proteasomes., *Methods Enzymol.* 398, 329-336.
38. Kabsch, W. (1993) Automatic processing of rotation diffraction data from crystals of initially unknown symmetry and cell constants., *J. Appl. Cryst.* 26, 795-800.
39. Brünger, A., Adams, P., Clore, G., DeLano, W., Gros, P., Grosse-Kunstleve, R., Jiang, J., Kuszewski, J., Nilges, M., Pannu, N., Read, R., Rice, L., Simonson, T., and Warren, G. (1998) Crystallography & NMR system: A new software suite for macromolecular structure determination., *Acta Crystallogr D Biol Crystallogr.* 1, 905-921.
40. Brünger, A. (1992) X-PLOR version 3.1. A system for X-ray crystallographie and NMR., *Yale University Press*, New Haven.

41. Turk, D. (1992) Improvement of a programm for molecular graphics and manipulation of electron densities and its application for protein structure determination, *Thesis*, Technische Universitaet Muenchen.
42. Groll, M., Ditzel, L., Lowe, J., Stock, D., Bochtler, M., Bartunik, H. D., and Huber, R. (1997) Structure of 20S proteasome from yeast at 2.4 Å resolution, *Nature* 386, 463-471.
43. Brünger, A. T. (1992) Free R value: a novel statistical quantity for assessing the accuracy of crystal structures, *Nature* 355, 472 - 475.
44. Groll, M., Huber, R., and Moroder, L. (2009) The persisting challenge of selective and specific proteasome inhibition, *J Pept Sci* 15, 58-66.
45. Ottmann, C., van der Hoorn, R. A., and Kaiser, M. (2012) The impact of plant-pathogen studies on medicinal drug discovery, *Chem Soc Rev* 41, 3168-3178.
46. Krahn, D., Ottmann, C., and Kaiser, M. (2011) The chemistry and biology of syringolins, glidobactins and cepafungins (syrbactins), *Nat Prod Rep* 28, 1854-1867.
47. Orlowski, R. Z., and Baldwin, A. S., Jr. (2002) NF-kappaB as a therapeutic target in cancer, *Trends Mol Med* 8, 385-389.
48. Kurland, J. F., and Meyn, R. E. (2001) Protease inhibitors restore radiation-induced apoptosis to Bcl-2-expressing lymphoma cells, *Int J Cancer* 96, 327-333.
49. Masdehors, P., Merle-Beral, H., Maloum, K., Omura, S., Magdelenat, H., and Delic, J. (2000) Deregulation of the ubiquitin system and p53 proteolysis modify the apoptotic response in B-CLL lymphocytes, *Blood* 96, 269-274.
50. Hideshima, T., Ikeda, H., Chauhan, D., Okawa, Y., Raje, N., Podar, K., Mitsiades, C., Munshi, N. C., Richardson, P. G., Carrasco, R. D., and Anderson, K. C. (2009)

1
2
3
4
5
6
7
8
9
10
11
12
13
14
15
16
17
18
19
20
21
22
23
24
25
26
27
28
29
30
31
32
33
34
35
36
37
38
39
40
41
42
43
44
45
46
47
48
49
50
51
52
53
54
55
56
57
58
59
60

Bortezomib induces canonical nuclear factor-kappaB activation in multiple myeloma cells, *Blood* 114, 1046-1052.

51. McConkey, D. J. (2009) Bortezomib paradigm shift in myeloma, *Blood* 114, 931-932.

52. Lowe, J., Stock, D., Jap, B., Zwickl, P., Baumeister, W., and Huber, R. (1995) Crystal structure of the 20S proteasome from the archaeon *T. acidophilum* at 3.4 Å resolution, *Science* 268, 533-539.

FIGURE LEGENDS

FIGURE 1: Chemical structures of SylA, GlbA, and the SylA-GlbA hybrid molecule.

(A) Syringolin A (SylA) is a natural product produced by the plant pathogen *Pseudomonas syringae* pv. *syringae* (*Pss*) and acts as a moderately potent proteasome inhibitor. (B)

Glidobactin A (GlbA) is a natural product proteasome inhibitor produced by an unknown species of the order *Burkholderiales* which is referred to as strain K481-B101 (ATCC 53080). (C) SylA-GlbA is a synthetic hybrid of SylA and GlbA.

1
2
3
4
5
6
7
8
9
10
11
12
13
14
15
16
17
18
19
20
21
22
23
24
25
26
27
28
29
30
31
32
33
34
35
36
37
38
39
40
41
42
43
44
45
46
47
48
49
50
51
52
53
54
55
56
57
58
59
60

FIGURE 2: SylA-GlbA inhibits proteasomal activities of tumor cells *in vivo*. A panel of human tumor cell lines including human multiple myeloma cell lines MM1.S (blue circles), MM1.RL (orange squares), and U266 (purple circles), human ovarian cancer cell line SKOV3 (green diamonds), and human neuroblastoma cell line SK-N-SH (red squares) were treated individually over a period of 2 hours with SylA-GlbA at various drug concentrations (0-10 μ M). The natural product wild type SylA and the FDA-approved proteasome inhibitor bortezomib (Velcade) were included as controls and tested in two cell lines (SK-N-SH, red squares and SKOV3, green diamonds). The inhibition of the chymotrypsin-like (CT-L), trypsin-like (T-L), and caspase-like (C-L) proteasome activity was determined by incubating treated cells with the bioluminescent substrates Suc-LLVY-aminoluciferin, Z-LRR-aminoluciferin, and Z-nLPnLD-aminoluciferin to measure the CT-L, T-L, and C-L proteasome activities, respectively. Data normalized to controls represent the mean of three independent experiments, and each experiment was performed in duplicate (n=6); *bars*, \pm SD. The CT-L activity measurements for GlbA, SylA, and bortezomib have been previously reported (24).

FIGURE 3: SylA-GlbA inhibits proliferation of tumor cells. A panel of human tumor cell lines including human multiple myeloma cell lines MM1.S (blue circles), MM1.RL (orange squares), and U266 (purple circles), human ovarian cancer cell line SKOV3 (green diamonds), and human neuroblastoma cell line SK-N-SH (red squares) were treated individually over a period of 48 hours with SylA-GlbA at various concentrations (0-1 μ M). The viability of cells was determined by MTS assay. Data normalized to controls represent the mean of three independent experiments, and each experiment was performed in triplicate (n=9); *bars*, SEM.

1
2
3
4
5
6
7
8
9
10
11
12
13
14
15
16
17
18
19
20
21
22
23
24
25
26
27
28
29
30
31
32
33
34
35
36
37
38
39
40
41
42
43
44
45
46
47
48
49
50
51
52
53
54
55
56
57
58
59
60

FIGURE 4: Structural characterization of SylA-GlbA. (A) Stereoview of $2F_o - F_c$ electron density map (grey mesh, 1σ) for the CT-L substrate binding channel in complex with SylA-GlbA (colored in green) which has been omitted prior phase calculations. The backbone of subunits $\beta 5$ and $\beta 6$ are presented in rose and grey coils, respectively; side chains involved in ligand stabilization are drawn in balls-and sticks-representation whereas hydrogen bonds are indicated by orange dashed lines. The lipophilic pocket stabilizing the aliphatic linker of SylA-GlbA is formed by Tyr-6, Pro94, Tyr96 and Pro115 from subunit $\beta 6$. Note, amino acid numbering of side chain residues is according to Loewe et al. (52). (B) Surface charge distribution shown for the CT-L active site. Surface colors indicate positive and negative electrostatic potentials contoured from 50 kT/e (intense blue) to -50 kT/e (intense red). Thr1 is colored in white and the inhibitor SylA-GlbA highlighted in green according to 4A. (C) Structural superposition of SylA-GlbA (green), GlbA (grey) and SylA (dark grey) bound to CT-L site. Thr1 of subunit $\beta 5$ is colored in black. The orientation is according to 4A.

Figure 1

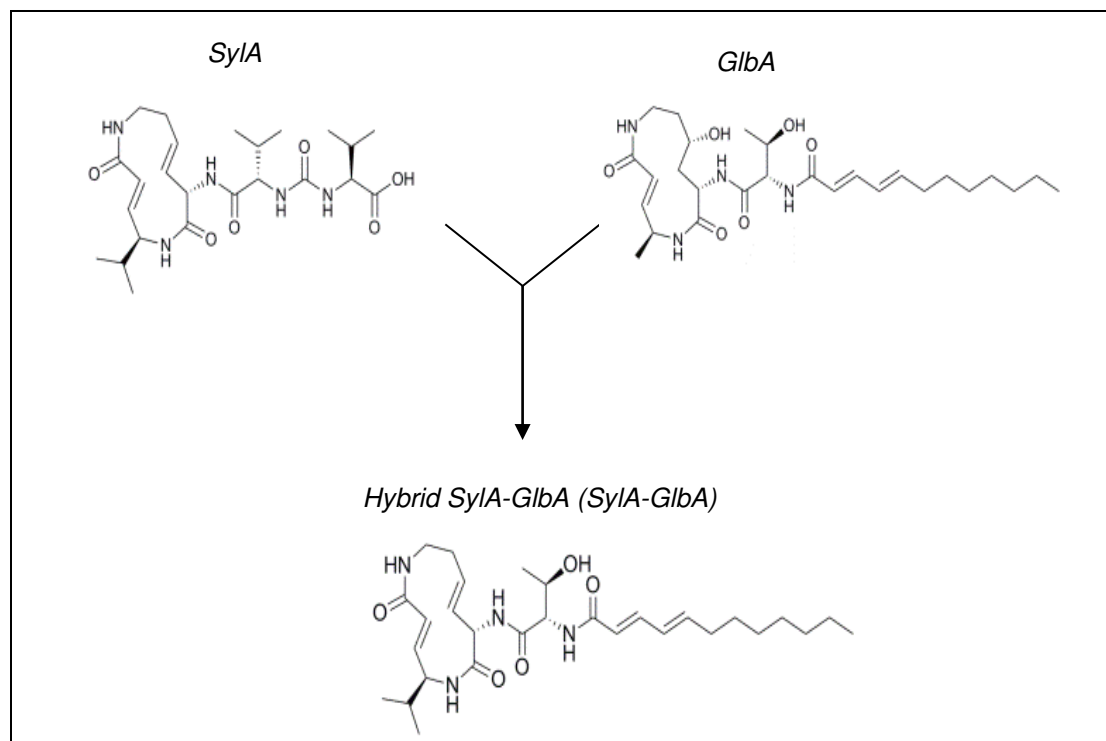


Figure 2

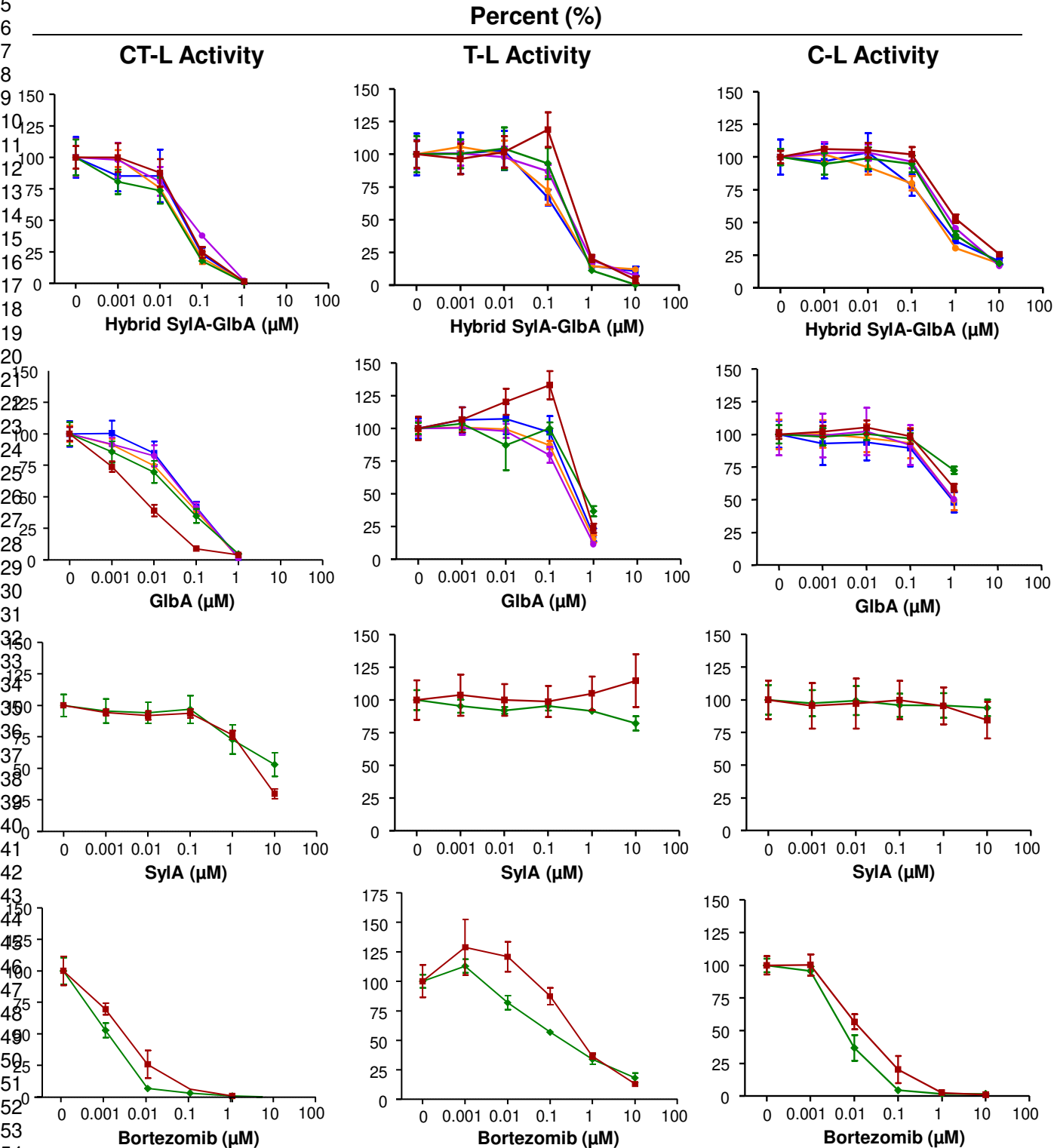


Figure 3

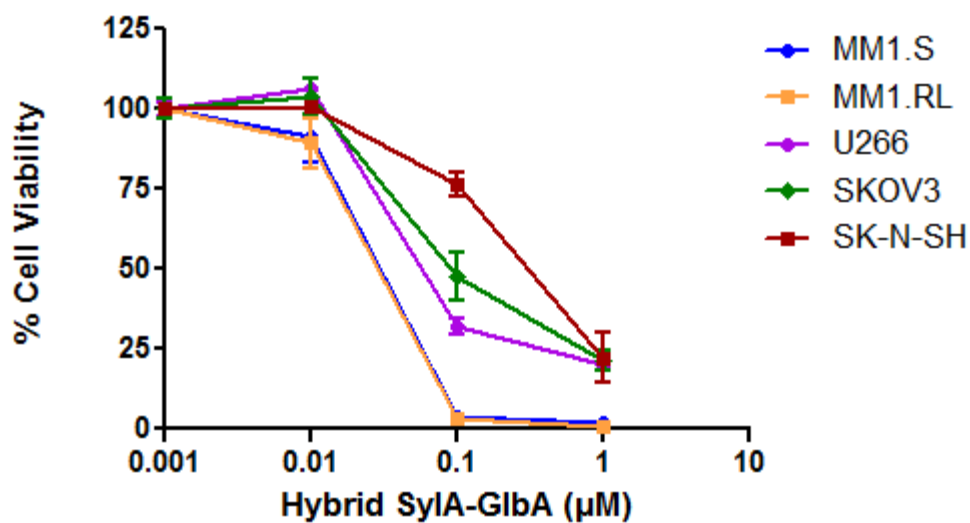


Figure 4

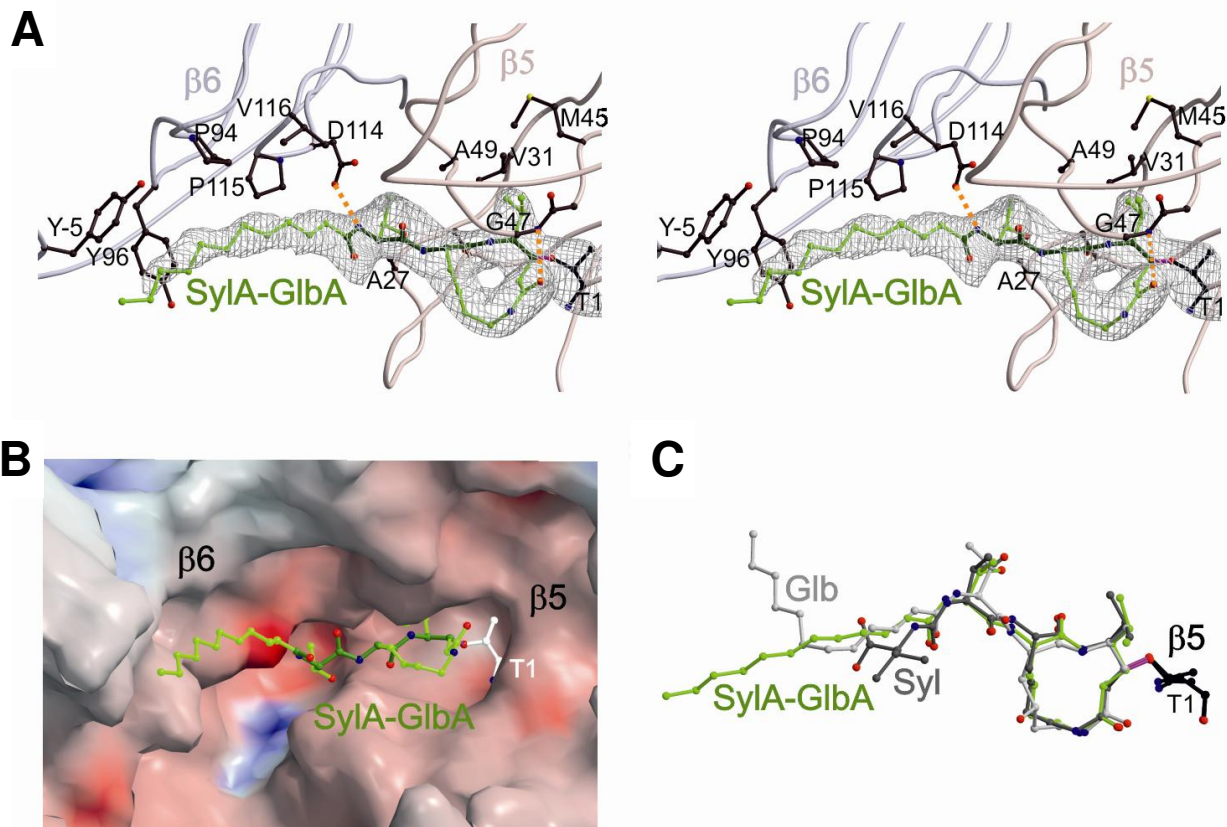


Table 1	
Cell viability	
IC ₅₀ values (nM)	
<i>Cell line</i>	<i>Hybrid SylA-GlbA</i>
MM1.S	28 ± 10
MM1.RL	27 ± 9
U266	45 ± 6
SKOV3	109 ± 111
SK-N-SH	321 ± 161

Table 2 Syrbactins inactivate NF-κB activity	
Compound	IC ₅₀ values (μM)*
Hybrid SylA-GIbA	2.87 ± 1.32
SylA	6.80 ± 2.00
GIbA	15.46 ± 2.90
TPCK (control 1)	4.2 ± 0.86
BAY-11 (control 2)	2.6 ± 0.12

*Dose-response curves based on eight serial dilutions of syrbactin compounds SylA-GIbA, SylA, and GIbA, and NFκB inhibitors TPCK and BAY-11 (positive controls) were used to determine the IC₅₀ values. Two independent experiments were performed in triplicate assays (n=6).